Genetic deletion of the kidney sodium/proton exchanger-3 (NHE3) does not alter calcium and phosphate balance due to compensatory responses

see commentary on page 222

OPEN

Søren B. Poulsen[1,7], Sathish K. Murali[1,2,7], Linto Thomas[3], Adrienne Assmus[1], Lena L. Rosenbæk[1], Rikke Nielsen[1], Henrik Dimke[4,5], Timo Rieg[3,6,7] and Robert A. Fenton[1,7]

[1]*Department of Biomedicine, Aarhus University, Aarhus, Denmark;* [2]*Department of Biomedical Sciences, University of Veterinary Medicine, Vienna, Austria;* [3]*Department of Molecular Pharmacology and Physiology, University of South Florida, Tampa, Florida, USA;* [4]*Department of Cardiovascular and Renal Research, Institute of Molecular Medicine, University of Southern Denmark, Odense, Denmark;* [5]*Department of Nephrology, Odense University Hospital, Odense, Denmark; and* [6]*James A. Haley Veterans' Hospital, Tampa, Florida, USA*

The sodium/proton exchanger-3 (NHE3) plays a major role in acid–base and extracellular volume regulation and is also implicated in calcium homeostasis. As calcium and phosphate balances are closely linked, we hypothesized that there was a functional link between kidney NHE3 activity, calcium, and phosphate balance. Therefore, we examined calcium and phosphate homeostasis in kidney tubule–specific NHE3 knockout mice (NHE3^{loxloxPax8} mice). Compared to controls, these knockout mice were normocalcemic with no significant difference in urinary calcium excretion or parathyroid hormone levels. Thiazide-induced hypocalciuria was less pronounced in the knockout mice, in line with impaired proximal tubule calcium transport. Knockout mice had greater furosemide-induced calciuresis and distal tubule calcium transport pathways were enhanced. Despite lower levels of the sodium/phosphate cotransporters (NaPi)-2a and -2c, knockout mice had normal plasma phosphate, sodium-dependent ^{32}Phosphate uptake in proximal tubule membrane vesicles and urinary phosphate excretion. Intestinal phosphate uptake was unchanged. Low dietary phosphate reduced parathyroid hormone levels and increased NaPi-2a and -2c abundances in both genotypes, but NaPi-2c levels remained lower in the knockout mice. Gene expression profiling suggested proximal tubule remodeling in the knockout mice. Acutely, indirect NHE3 inhibition using the SGLT2 inhibitor empagliflozin did not affect urinary calcium and phosphate excretion. No differences in femoral bone density or architecture were detectable in the knockout mice. Thus, a role for kidney NHE3 in calcium homeostasis can be unraveled by diuretics, but NHE3 deletion in the kidneys has no major effects on overall calcium and phosphate homeostasis due, at least in part, to compensating mechanisms.

Kidney International (2025) **107,** 280–295; https://doi.org/10.1016/j.kint.2024.07.013

KEYWORDS: blood pressure; calcium; gliflozins; parathyroid hormone; phosphate; proximal tubule

Translational Statement

Understanding mechanisms maintaining Ca^{2+} and P_i homeostasis has implications for disease management. The Na^+/H^+ exchanger-3 (NHE3) in the proximal tubule is proposed to be important for Ca^{2+} transport, and Ca^{2+} and P_i homeostasis are closely linked by hormonal regulators. Here we demonstrate that inhibition of kidney NHE3 does not affect overall P_i or Ca^{2+} homeostasis, and reduced proximal tubule Ca^{2+} reabsorption is compensated for by distal segments. This suggests that drugs affecting renal NHE3 activity (e.g., NHE3 inhibitors or gliflozins) are unlikely to result in Ca^{2+} and P_i sequela in the absence of therapies that affect distal Ca^{2+} transport mechanisms.

Approximately 10 to 15 mm Hg of basal blood pressure has been attributed to kidney Na^+/H^+ exchanger-3 (NHE3) activity. As such, pharmacologic inhibition of renal NHE3 has been proposed as a clinically relevant strategy for treating hypertension. Supporting this concept, lower blood pressure is observed in mice lacking NHE3 in the whole kidney or the renal proximal tubule (PT)[1–4] and deletion of NHE3, or administration of an orally absorbable NHE3 inhibitor also alleviates approximately 50% of angiotensin II–induced hypertension.[3] Furthermore, NHE3 and the sodium-glucose transporter 2 (SGLT2) functionally interact in the PT, and a reduction in NHE3 activity subsequent to

Correspondence: *Robert A. Fenton, Institute for Biomedicine, Aarhus University, Wilhelm Meyers Allé 3, Building 1233, DK-8000 Aarhus C, Denmark. E-mail: robert.a.fenton@biomed.au.dk; or Timo Rieg, Department of Molecular Pharmacology and Physiology, Morsani College of Medicine, University of South Florida, 12901 Bruce B. Downs Blvd, MDC8, Tampa, Florida 33612, USA. E-mail: trieg@usf.edu*

[7]SBP, SKM, TR, and RAF contributed equally to this work.

Received 5 July 2022; revised 10 June 2024; accepted 2 July 2024; published online 30 July 2024

SGLT2 inhibition may underlie, at least in part, the antihypertensive effect of empagliflozin or other SGLT2 inhibitors.[5–8] However, NHE3 may also be important for renal Ca^{2+} handling,[9] and understanding how inhibition of NHE3 in the kidney impacts this process is therefore of clinical significance.

In the PT, approximately 70% of filtered Ca^{2+} is reabsorbed via paracellular transport, and this is primarily facilitated by the exchange of luminal Na^+ ions for intracellular H^+ by NHE3.[9–11] The importance of PT transport for driving Ca^{2+} reabsorption is also clinically important to increase Ca^{2+} reabsorption in response to treatment with thiazide diuretics,[12] and the mechanism remains a cornerstone of kidney Ca^{2+} transport described in textbooks. However, PT NHE3 is also acutely and chronically inhibited in response to parathyroid hormone (PTH) via a variety of mechanisms,[13–17] and increased $NaHCO_3$ delivery to the distal tubule may contribute to enhance Ca^{2+} reabsorption.[18–20]

Ca^{2+} and phosphate (P_i) homeostasis are closely linked, with PTH, 1,25-dihydroxyvitamin D3 (1,25$(OH)_2$ D_3, vitamin D [vitD]), and fibroblast growth factor 23 (FGF23) working in concert to maintain Ca^{2+} and P_i homeostasis.[10,21–23] In addition to regulation of NHE3, these hormones alter the activity of the kidney Na^+-Pi cotransporter (NaPi)-2a and -2c to modulate urinary P_i excretion, and NHE3 and NaPi-2a can be regulated by the same scaffolding proteins such as Na^+/H^+ exchanger regulatory factor[10,21,24–33] and PDZ domain containing 1.[34] Therefore, we hypothesized that there would be a functional link between kidney NHE3 activity and Ca^{2+} and P_i handling. To assess this, we investigated the impact of long-term kidney NHE3 "inhibition" on Ca^{2+} and P_i homeostasis using kidney tubule–specific NHE3 knockout (KO) mice ($NHE3^{loxloxPax8}$ mice).[1,35]

CONDENSED METHODS

Study approval

All experiments on kidney-specific NHE3 KO ($NHE3^{loxloxPax8}$) mice were conducted in accordance with rules from local authorities.

Generation of the kidney-specific NHE3 KO mouse model

$NHE3^{loxlox}$ mice (termed control mice) and $NHE3^{loxloxPax8}$ mice were generated as described.[35] Mice were housed under a 12:12 hour light:dark cycle in standard rodent cages with free access to water and rodent chow (0.8% NaCl, TD.7001 or TD.2018, Harlan Teklad). Experimental mice were 3 to 6 months old. The sex of the mice (male or female) used in each experiment is specified in the figure legends.

Furosemide and thiazide response experiments

Control and $NHE3^{loxloxPax8}$ mice were administered hydrochlorothiazide (HTZ, oral gavage, 25 mg/kg in 5% Cremophor, 10% dimethylsulfoxide, and 85% H_2O; 10 µl/g body weight) or furosemide (intraperitoneal injection, 25 mg/kg in 0.9% saline; 1 µl/g body weight). After administration, mice were transferred to metabolic cages (Tecniplast; without access to water and food) in which urine was collected over 30-minute periods.[36]

Low-P_i diet experiment

Male control and $NHE3^{loxloxPax8}$ mice were fed a control diet (0.7% P_i thereof 0.4% non-phytate P_i; TD.2018, Envigo) for 1 week before half of the mice were switched to a low-P_i diet (<0.01% P_i; TD.08601, Envigo) for 1 week before analysis; see Supplementary Extended Methods.

Collection and analyses of blood and urine

Blood was drawn from the retro-orbital plexus. Urine was collected either as spot urine or in metabolic cages. Analysis is described in the Supplementary Extended Methods.

Immunoblotting

See Supplementary Extended Methods. Antibodies are listed in Supplementary Table S1. Coomassie-stained gels were used to correct quantification for deviations in protein loading (Supplementary Figure S1).

RNA extraction and reverse transcription quantitative polymerase chain reaction

See Supplementary Extended Methods. Primer sequences are listed in Supplementary Table S2.

Immunohistochemistry and proximity ligation assays

See Supplementary Extended Methods. Antibodies are listed in Supplementary Table S1.

Statistics

Densitometry data were tested for normality and variance homogeneity as described in Supplementary Extended Methods. All *P* values for multiple comparisons within and between groups were adjusted using Benjamini-Yekutieli false discovery rate correction. Values are presented as individual data points and mean ± SEM.

Clearance experiments, ^{33}P intestinal uptakes, microscopy, fecal P_i and Ca^{2+} excretion, bone analysis by peripheral quantitative computed tomography, and brush border membrane vesicle (BBMV) uptakes are described in Supplementary Extended Methods.

RESULTS

Male $NHE3^{loxloxPax8}$ mice have normal plasma Ca^{2+} and urinary Ca^{2+} excretion at baseline

By Western blotting, NHE3 was virtually undetectable in the kidneys of $NHE3^{loxloxPax8}$ mice (Figure 1a). Immunohistochemistry (Supplementary Figure S2) demonstrated that in the cortex of $NHE3^{loxloxPax8}$ mice, NHE3 was sparingly expressed in a few cells in the PT and the thick ascending limb (TAL). In the outer stripe of outer medulla, some TAL cells expressed NHE3 with an intensity comparable to control mice, but this event was sparse. Kidneys from $NHE3^{loxloxPax8}$ mice appeared structurally normal with no evidence of renal injury, tubular damage, or apoptosis (Supplementary Figure S3). Total and ionized plasma Ca^{2+} levels were similar between genotypes, and there were no

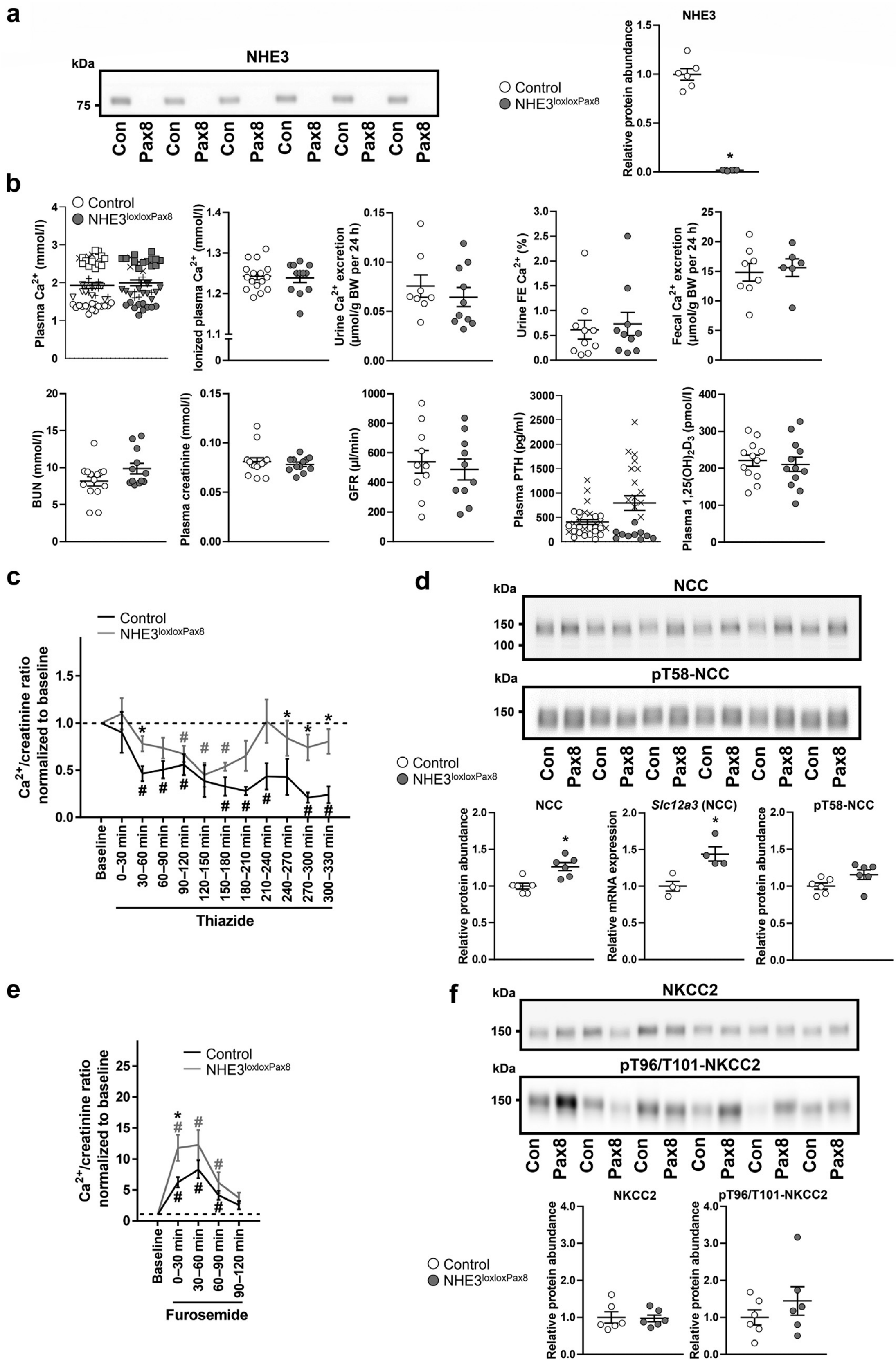

Figure 1 | Effects of renal sodium/proton exchanger-3 (NHE3) deletion on Ca^{2+} homeostasis can be unraveled by diuretics. (**a**) Western blotting and corresponding densitometry analysis of NHE3 abundance in whole kidney homogenates from control and NHE3^{loxloxPax8} mice (n = 6 per genotype). (**b**) Relative to controls, NHE3^{loxloxPax8} mice had normal levels of plasma Ca^{2+}, ionized plasma Ca^{2+}, 24-hour urinary Ca^{2+} excretion, fractional excretion (FE) of Ca^{2+}, fecal Ca^{2+} excretion, blood urea nitrogen (BUN), plasma creatinine, glomerular (continued) significant differences in 24-hour urinary Ca^{2+} excretion, fractional Ca^{2+} excretion, blood urea nitrogen, or plasma creatinine levels (Figure 1b and Supplementary Figure S4A and B). Other baseline physiological parameters are depicted in Supplementary Figure S5. Using fluorescein isothiocyanate–sinistrin clearance, no significant differences in glomerular filtration rate were detectable between the genotypes (Figure 1b). $NHE3^{loxloxPax8}$ mice had modestly increased plasma PTH compared with controls ($P = 0.06$), but no differences in plasma vitD concentrations (Figure 1b and Supplementary Figure S4C) or mRNA levels of *Cyp24a1* and *Cyp27b1*, enzymes involved in vitD metabolism (Supplementary Figure S5). Similar results for plasma Ca^{2+}, PTH, and vitD were obtained from female mice (Supplementary Figure S6).

Reduced PT Ca^{2+} reabsorption in $NHE3^{loxloxPax8}$ mice

Overall Ca^{2+} balance did not appear to be affected in the $NHE3^{loxloxPax8}$ mice, indicating that either kidney NHE3 is not important for maintaining Ca^{2+} homeostasis or compensatory mechanisms have developed. To test the first possibility, mice were given a single bolus injection of HTZ and urinary Ca^{2+} excretion assessed. The reasoning behind this approach was that if HTZ causes hypocalciuria by increasing NHE3-mediated paracellular Ca^{2+} reabsorption subsequent to volume depletion,[12,37–41] then lack of NHE3 would result in greater Ca^{2+} excretion compared with controls. Both genotypes reduced urine osmolality and urinary Ca^{2+} excretion in response to HTZ, but the overall reduction and the timeframe of reduced Ca^{2+} excretion were attenuated in $NHE3^{loxloxPax8}$ mice (Figure 1c and Supplementary Figure S7). These results indicate that HTZ-induced hypocalciuria is partially dependent on NHE3, but also that there is less PT Ca^{2+} reabsorption in $NHE3^{loxloxPax8}$ mice under baseline conditions. Although their Ca^{2+} handling responses to HTZ were reduced, $NHE3^{loxloxPax8}$ mice had greater mRNA, protein, and phosphorylation levels of the thiazide-sensitive NaCl cotransporter than control mice (Figure 1d).

Enhanced Ca^{2+} reabsorption in TAL of $NHE3^{loxloxPax8}$ mice

The paracellular Ca^{2+} pathway in the TAL accounts for approximately 20% of filtered Ca^{2+} reabsorption.[10,42–46] This pathway is highly dependent on NKCC2-driven lumen-positive voltage. To assess if the enhancement of this pathway could contribute to normal Ca^{2+} homeostasis in the $NHE3^{loxloxPax8}$ mice, mice were given a single bolus injection of furosemide and urinary Ca^{2+} excretion was examined over a subsequent 2-hour period. Furosemide decreased urine osmolality and increased urinary Ca^{2+} excretion in both genotypes (Figure 1e and Supplementary Figure S8). However, the increase in urinary Ca^{2+} excretion was significantly greater in $NHE3^{loxloxPax8}$ mice relative to controls, as emphasized by the area under the curve being approximately 60% larger. By Western blotting (Figure 1f) and quantitative confocal microscopy (Supplementary Figure S9), total and T96/T101 phosphorylated NKCC2 protein abundances were not different between the genotypes. However, $NHE3^{loxloxPax8}$ mice had significantly greater S126 phosphorylated NKCC2 levels (Supplementary Figure S9). Together these data suggest a higher contribution of the TAL to Ca^{2+} reabsorption in the $NHE3^{loxloxPax8}$ mice.

Claudin-16 in the TAL allows permeation of paracellular Ca^{2+},[47,48] whereas Claudin-14 expression is markedly stimulated by the activation of the calcium-sensing receptor and plays an important role in adjusting Ca^{2+} transport in the TAL.[49,50] Claudin-14 was undetectable in control and $NHE3^{loxloxPax8}$ mice under basal conditions (Figure 2a).[49,50] Claudin-16 was detectable in basolateral membrane domains and tight junctions of TALs as described previously,[47,48] and overall staining intensity did not appear to differ between genotypes (Figure 2b). Supporting this, *Cldn16* mRNA expression was not different between the groups (mean ± SEM [n]; control: 1.0 ± 0.1 [5], $NHE3^{loxloxPax8}$: 1.2 ± 0.1 [5], $P > 0.05$).

Increased expression of transcellular Ca^{2+} transport pathways in the distal nephron

The distal convoluted tubule (DCT) and the connecting tubule reabsorb approximately 10% of filtered Ca^{2+} via transcellular transport.[10] To assess if enhanced Ca^{2+} reabsorption in these segments may exist in $NHE3^{loxloxPax8}$ mice, the levels of various Ca^{2+} transport pathways were evaluated. Protein and mRNA levels of the calcium-selective channel transient receptor potential cation channel subfamily V member 5 (TRPV5) were greater in $NHE3^{loxloxPax8}$ mice than controls (Figure 2c), whereas no significant differences were detected in the levels of the calcium-binding protein calbindin D-28k (Figure 2d). At the mRNA level, $NHE3^{loxloxPax8}$ mice had greater expression of *Trpv6*, but there were no significant differences in the expression of *CaBP-9k* (calbindin-D9k [CaBP9k]), *Pvalb* (parvalbumin), *Atp2b1* (plasma membrane Ca^{2+} ATPase 1), *Atp2b4* (plasma membrane Ca^{2+} ATPase 4), and *Slc8a1* (Na^+/Ca^{2+} exchanger 1; Figure 2e).

Figure 1 | (continued) filtration rate (GFR), plasma parathyroid hormone (PTH), and plasma $1,25(OH)_2 D_3$ (n = 8–48 mice per genotype). For plasma Ca^{2+} and PTH, matching symbols represent different animal cohorts. (**c**) Urinary Ca^{2+}/creatinine ratio decreased in both genotypes after the injection of hydrochlorothiazide (HTZ) but was attenuated in $NHE3^{loxloxPax8}$ mice (n = 6–9 per genotype). (**d**) Analyses of the NaCl cotransporter (NCC), phosphorylated (pT58) NCC, and NCC and NCC mRNA in $NHE3^{loxloxPax8}$ mice relative to controls (n = 4–6 per genotype). (**e**) Urinary Ca^{2+}/creatinine ratio in both control and $NHE3^{loxloxPax8}$ mice increased after furosemide administration (n = 10 per genotype) but was significantly greater in $NHE3^{loxloxPax8}$ mice between 0 and 30 minutes, suggesting higher baseline NKCC2-mediated Ca^{2+} reabsorption. (**f**) Western blotting and corresponding densitometry analyses of NKCC2 and pT96-T101-NKCC2 protein abundance. Data in panels (**a**), (**b**), (**d**), and (**f**) are from male mice. Data in panels (**c**) and (**e**) are from a mixed male and female cohort. Values are mean ± SEM, and individual data points are shown where feasible. Statistical analyses were performed using appropriate pairwise comparison tests (**a,b,d,f**) or paired or pairwise comparison tests followed by Benjamini-Yekutieli false discovery rate correction (**c,e**). *$P < 0.05$ between genotypes. $^{\#}P < 0.05$ versus baseline same genotype. BW, body weight.

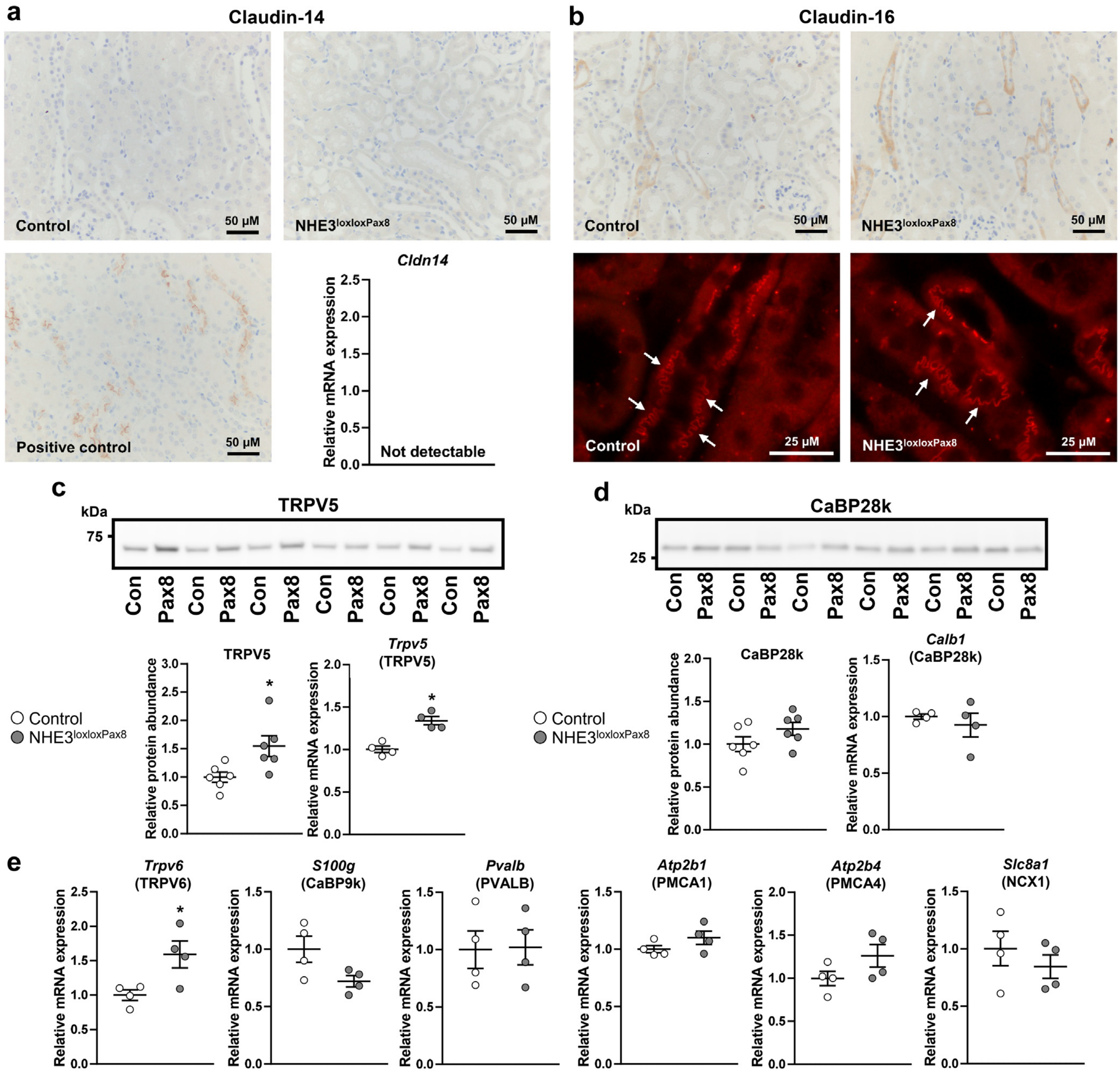

Figure 2 | Sodium/proton exchanger-3 (NHE3)^{loxloxPax8} mice show no difference in claudin-14 and -16 but have greater transient receptor potential cation channel subfamily V member 5 (TRPV5) and TRPV6 levels. (**a**) Claudin-14 was absent in control and NHE3^{loxloxPax8} mice under basal conditions (n = 6 per genotype), but detectable in tissue from mice with dihydrotachysterol-induced hypercalcemia (positive control).[49,50] mRNA levels were not detectable in the kidney of either genotype (n = 5 per genotype). (**b**) Claudin-16 was detectable in basolateral membrane domains and the tight junction of control and NHE3^{loxloxPax8} mice (see arrows). Overall, expression levels did not appear to differ between the genotypes, but variability in staining intensity was seen in both groups. (**c**) NHE3^{loxloxPax8} mice have greater TRPV5 protein and mRNA abundances than control mice (n = 4–6 per genotype). (**d**) Between genotypes, no differences were found in protein and mRNA abundances of calcium-binding protein calbindin D-28k (CaBP-D28k; n = 4–6 per genotype). (**e**) Relative to controls, the mRNA levels of TRPV6 were greater in NHE3^{loxloxPax8} mice, but no significant differences were found in CaBPD9k, PVALB, PMCA1, PMCA4, or NCX1 (n = 4 per genotype). Data in all panels are from male mice. Values are mean ± SEM and individual data points. Statistical analyses were performed using appropriate pairwise comparison tests. *$P < 0.05$ versus control. To optimize viewing of this image, please see the online version of this article at www.kidney-international.org.

Plasma P_i levels, intestinal P_i handling, and P_i uptake in kidney BBMVs are similar in NHE3^{loxloxPax8} mice despite reduced NaPi-2a and -2c

Plasma P_i was comparable in male control and NHE3^{loxloxPax8} mice, and no difference was observed in 24-hour urinary P_i excretion, fractional P_i excretion, or plasma FGF-23 levels (Figure 3a and Supplementary Figure S10). Similar observations on plasma P_i were obtained in female mice, although they displayed mildly elevated FGF23 (Supplementary Figure S11). Surprisingly, NaPi-2a protein levels were lower

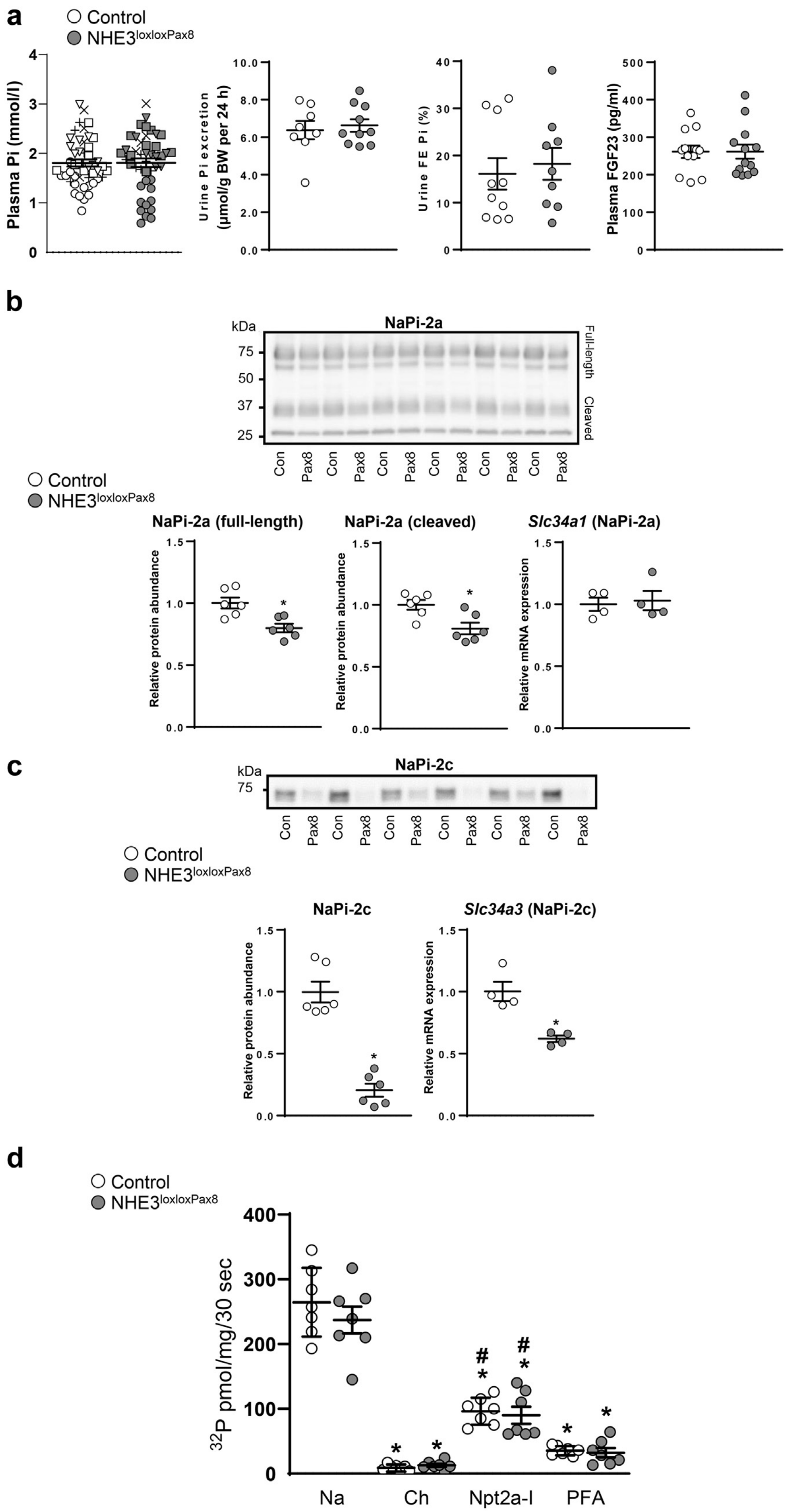

Figure 3 | Sodium/proton exchanger-3 (NHE3)^{loxloxPax8} mice have lower sodium/phosphate cotransporters-2a (NaPi-2a) and -2c abundances but unchanged Na$^+$-dependent P_i uptake in brush border membrane vesicles (BBMVs) and normal plasma P_i. (**a**) Relative to controls, NHE3^{loxloxPax8} mice had normal plasma P_i (matching symbols represent different animal cohorts), urine P_i excretion, urinary fractional excretion (FE) of P_i, and plasma fibroblast growth factor 23 (FGF23) levels (n = 8–47 per genotype). (**b**) Western blots (continued) in male NHE3^{loxloxPax8} mice independent of mRNA changes, whereas there was a large reduction in NaPi-2c protein and mRNA abundance (Figure 3b and c). Normal P_i balance in NHE3^{loxloxPax8} mice, despite the lower NaPi-2a and -2c, could not be attributed to increased intestinal P_i absorption, as plasma ^{33}P levels 120 minutes after ^{33}P oral gavage were not significantly different between genotypes (Figure 4a and Supplementary Figure S12). Supporting this, fecal P_i excretion (Figure 4b) and staining intensity and distribution of NaPi-2b throughout the intestine were equivalent between genotypes (Figure 4c).

To assess the functional impact of the reduced NaPi-2a and -2c, we analyzed P_i transport across isolated kidney BBMVs. Na^+-dependent ^{32}P uptake, Na^+-independent uptake, NaPi-2a-mediated uptake, or NaPi-2a/c-mediated uptake was not significantly different between genotypes (Figure 3d). Of note, despite greater mRNA for the type III inorganic P_i transporter PiT-1 in NHE3^{loxloxPax8} mice (Supplementary Figure S13), no significant differences were observed between BBMVs treated with phosphonoformic acid (inhibitor of NaPi cotransporters) and Na^+-free conditions, consistent with the majority of BBMV-mediated P_i uptake being Na^+-dependent.[51]

To assess if the abundances of NaPi-2a and -2c could still adapt to dietary P_i challenges in the absence of kidney NHE3, mice were fed a low-P_i diet for 7 days. In both genotypes, a low-P_i diet resulted in lower urinary P_i excretion, plasma P_i, PTH, and FGF23 levels, but no significant differences between genotypes were found (Figure 5a). NaPi-2a and -2c protein levels were significantly greater after a low-P_i intake in both genotypes (Figure 5b). In contrast to the standard diet, no significant differences were found between the genotypes in NaPi-2a protein abundance on the low-P_i diet. However, NaPi-2c protein abundance remained significantly lower in the NHE3^{loxloxPax8} mice on the low-P_i diet. On the low-P_i diet, NaPi-2a and -2c mRNA levels were greater than the standard diet in both genotypes, but the significantly lower levels of NaPi-2c mRNA relative to controls were still apparent (Figure 5c).

PT remodeling in NHE3^{loxloxPax8} mice may contribute to reductions in NaPi-2c

In order to explain the reductions in NaPi-2a and -2c in the NHE3^{loxloxPax8} mice, we initially focused on the observations that Na^+/H^+ exchanger regulatory factor and PDZ domain containing 1 interact with NaPi-2a and -2c and NHE3 to alter their cellular distribution,[24–30,52,53] with the hypothesis that deleting NHE3 may thus impair a macromolecular complex and alter NaPi-2a and -2c distribution and degradation kinetics.[54,55] In support of this concept, NHE3 and NaPi-2a colocalized at the apical brush border of control mice (Figure 6a), and NaPi-2a and NHE3 could be co-immunoprecipitated in protein lysates from *ex vivo* kidney cortical tubule suspensions (Figure 6b). Furthermore, proximity ligation assays performed on mouse kidney sections indicate that NHE3 and NaPi-2a are closely associated (<40 nm apart[56]), with numerous punctae in PTs indicating NHE3:NaPi-2a protein-protein interactions (Figure 6c). However, in kidney sections from control and NHE3^{loxloxPax8} mice, no clear differences in NaPi-2a and -2c subcellular localization could be observed between the genotypes (Figure 6d and e). Furthermore, although there were a significantly lower number of NaPi-2c positive cells in NHE3^{loxloxPax8} mice than controls (Supplementary Figure S14), NaPi-2c was undetectable in some cells that showed NHE3 expression due to incomplete gene deletion (Figure 6f), suggesting that NHE3 is not a prerequisite for NaPi-2c expression. No differences were detectable in the cellular localization of Na^+/H^+ exchanger regulatory factor or PDZ domain containing 1 in the NHE3^{loxloxPax8} mice, but they were significantly reduced in abundance at the protein level (Supplementary Figure S15).

Mathematical modeling and experimental data indicate that after NHE3 deletion or use of SGLT2 inhibitors, there is a shift in Na^+ reabsorption to downstream nephron segments, including the S3 segment.[7,57,58] To examine whether, at least in part, structural and/or functional adaptation in the PT contributes to the greatly reduced NaPi-2c abundance in NHE3^{loxloxPax8} mice, we examined the mRNA expression profile of 19 genes with a differential distribution along the mouse PT using reverse transcription quantitative polymerase chain reaction.[59–61] As observed in the heatmap (Figure 6g), the expression of genes associated with the S1 segment of the PT are lower in NHE3^{loxloxPax8} mice than control mice, whereas the expression of genes associated with the S2 and S3 segment are higher, suggesting a reduction in the length of S1 in the NHE3^{loxloxPax8} mice.

NHE3^{loxloxPax8} mice have normal long-bone architecture

The majority of total body Ca^{2+} and P_i are stored in bone, and imbalances of these minerals alter bone metabolism. Analysis of femoral bone from control and NHE3^{loxloxPax8} mice by peripheral quantitative computed tomography revealed no significant changes in total volumetric bone mineral density (total BMD), cortical BMD, and cortical thickness in the midshaft region (Figure 7a). The

Figure 3 | (continued) of whole kidney demonstrated significantly lower full-length (approximately 75 kDa) and cleaved NaPi-2a (approximately 37 kDa) in NHE3^{loxloxPax8} than control mice (n = 6 per genotype). No significant differences were found in NaPi-2a mRNA levels (n = 4 per genotype). (**c**) NHE3^{loxloxPax8} mice had lower NaPi-2c protein and mRNA compared with control mice (n = 4–6 per genotype). (**d**) In BBMVs, Na^+-dependent ^{32}P uptake, Na^+-independent uptake (balanced using choline Cl^-, Ch), NaPi-2a-mediated uptake (Npt2a-I), or Npt2a/c-mediated uptake (phosphonoformic acid [PFA]) was not significantly different between genotypes. Data in all panels are from male mice. Values are mean ± SEM and individual data points. Statistical analyses were performed using appropriate pairwise comparison tests (**a–c**), where $^*P < 0.05$ between genotypes, or 2-way analysis of variance followed by Tukey's multiple comparisons test (**d**) where $^*P < 0.05$ versus Na^+ same genotype, $\#P < 0.05$ versus Na^+, choline, and PFA same genotype. BW, body weight.

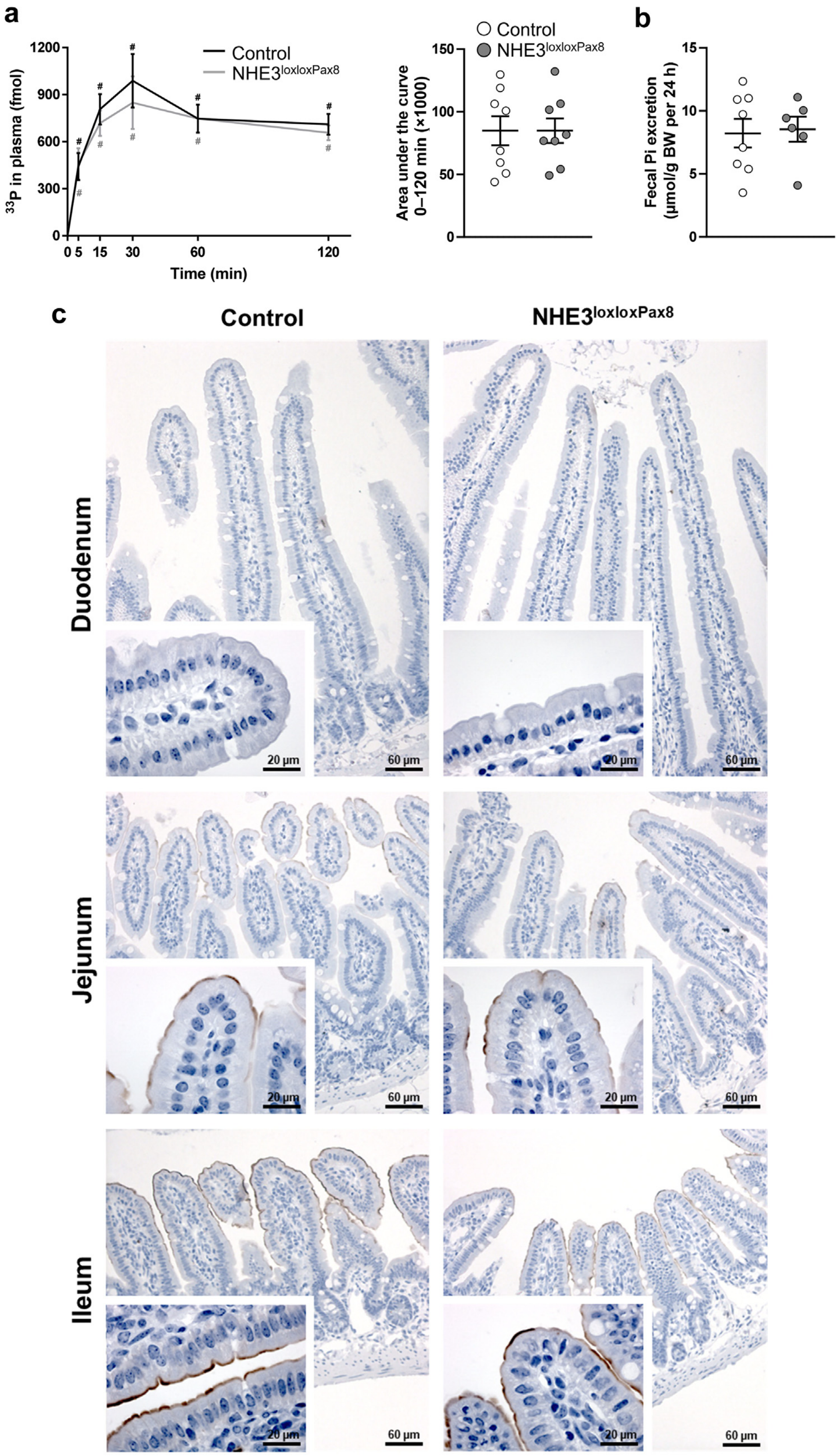

Figure 4 | Normal intestinal P_i handling in sodium/proton exchanger-3 (NHE3)^{loxloxPax8} mice. (**a**) Control and NHE3^{loxloxPax8} mice were administered ^{33}P via oral gavage, and subsequently plasma levels of ^{33}P were followed over 120 minutes. There were no significant differences in plasma ^{33}P levels between genotypes, and the areas under the curve are approximately equal, suggesting comparable P_i handling (n = 7–8 per genotype). (**b**) Fecal P_i excretion was equivalent between genotypes (n = 6–8 per genotype). (**c**) Immunohistochemical (continued)

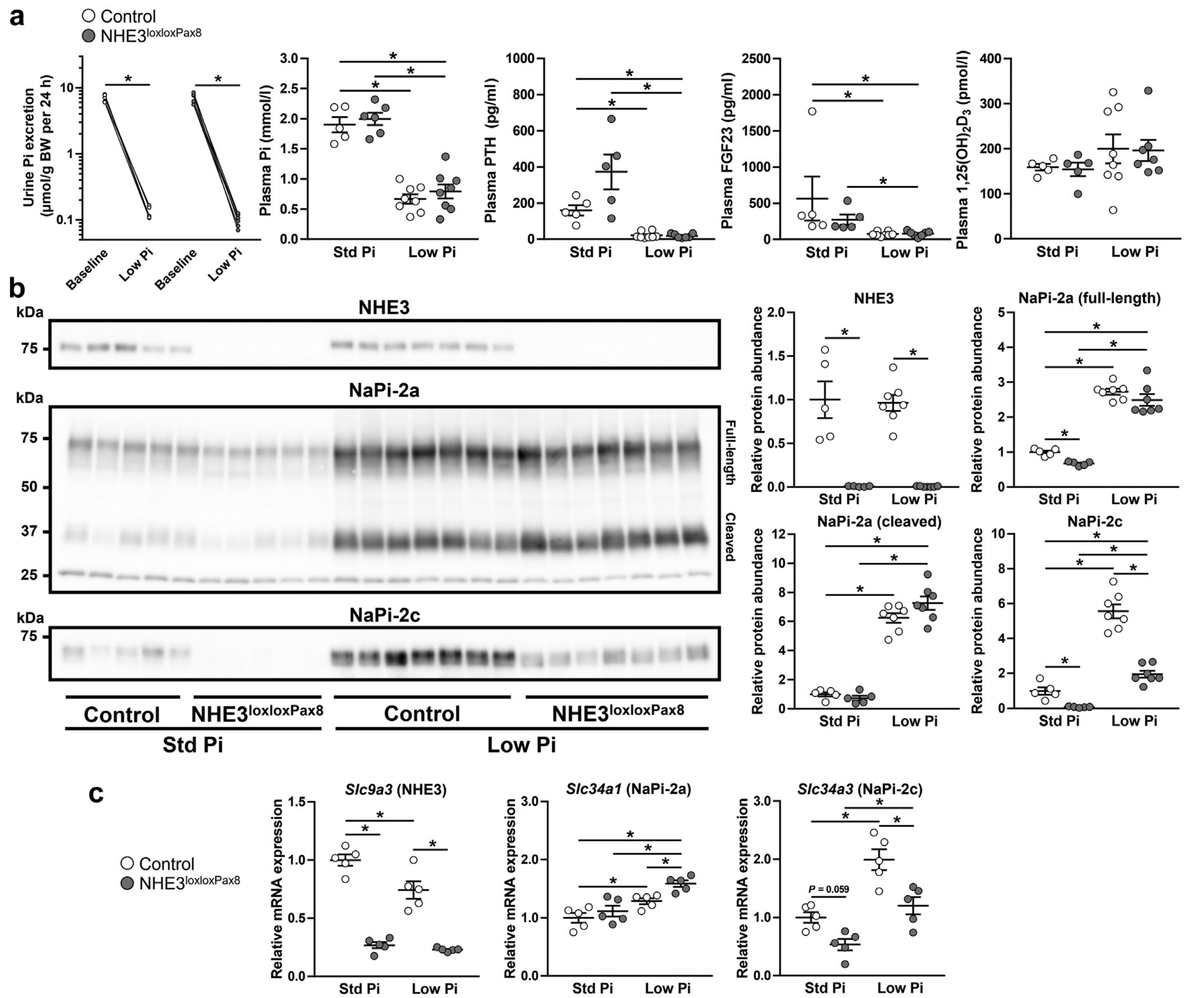

Figure 5 | On a low-P_i diet, sodium/proton exchanger-3 (NHE3)^{loxloxPax8} mice increase sodium/phosphate cotransporters-2a (NaPi-2a) and -2c protein abundance and reduce urinary P_i excretion. (**a**) A low-P_i diet decreased urinary P_i excretion, plasma P_i, plasma parathyroid hormone (PTH), and plasma fibroblast growth factor 23 (FGF23) in both control and NHE3^{loxloxPax8} mice. Urinary P_i excretion was comparable between the genotypes (n = 5–8 per genotype). (**b**) In NHE3^{loxloxPax8} mice, the low-P_i diet increased NaPi-2a (full-length [approximately 75 kDa] and cleaved [approximately 37 kDa]) and NaPi-2c protein abundances relative to a standard (Std) diet. However, NaPi-2c protein abundance was still significantly less in the NHE3^{loxloxPax8} mice relative to control mice when fed the low-P_i diet (n = 5–7 per genotype). (**c**) The low-P_i diet increased NaPi-2a and -2c mRNA expression levels in both control and NHE3^{loxloxPax8} mice (n = 5 per genotype). Data in all panels are from male mice. Values are mean ± SEM and individual data points. Statistical analyses were performed using a 2-way repeated measures analysis of variance (ANOVA) (**a**) or a 2-way ANOVA followed by Holm-Sidak *post hoc* tests and Benjamini-Yekutieli false discovery rate correction (**a–c**). *$P < 0.05$ versus control. BW, body weight.

cross-sectional areas of the midshaft region were also similar between the groups, with no significant changes in periosteal and endosteal circumferences (Figure 7a). In the distal metaphysis, the total BMD and cortical BMD were not significantly different between genotypes (Figure 7b). Trabecular bone in the distal metaphysis had no significant changes in trabecular BMD, trabecular area, or trabecular content between genotypes (Figure 7b). Together, these data support that renal NHE3 deletion does not alter overall bone health.

Figure 4 | (continued) labeling showed no detectable differences in staining intensity or distribution of sodium/phosphate cotransporters-2b (NaPi-2b) throughout the small intestine (n = 4 per genotype). Data in all panels are from male mice. Statistical analyses were performed using appropriate paired or pairwise comparison tests followed by Benjamini-Yekutieli false discovery rate correction. Values are mean ± SEM and individual data points. $^{\#}P < 0.05$ versus baseline same genotype. BW, body weight. To optimize viewing of this image, please see the online version of this article at www.kidney-international.org.

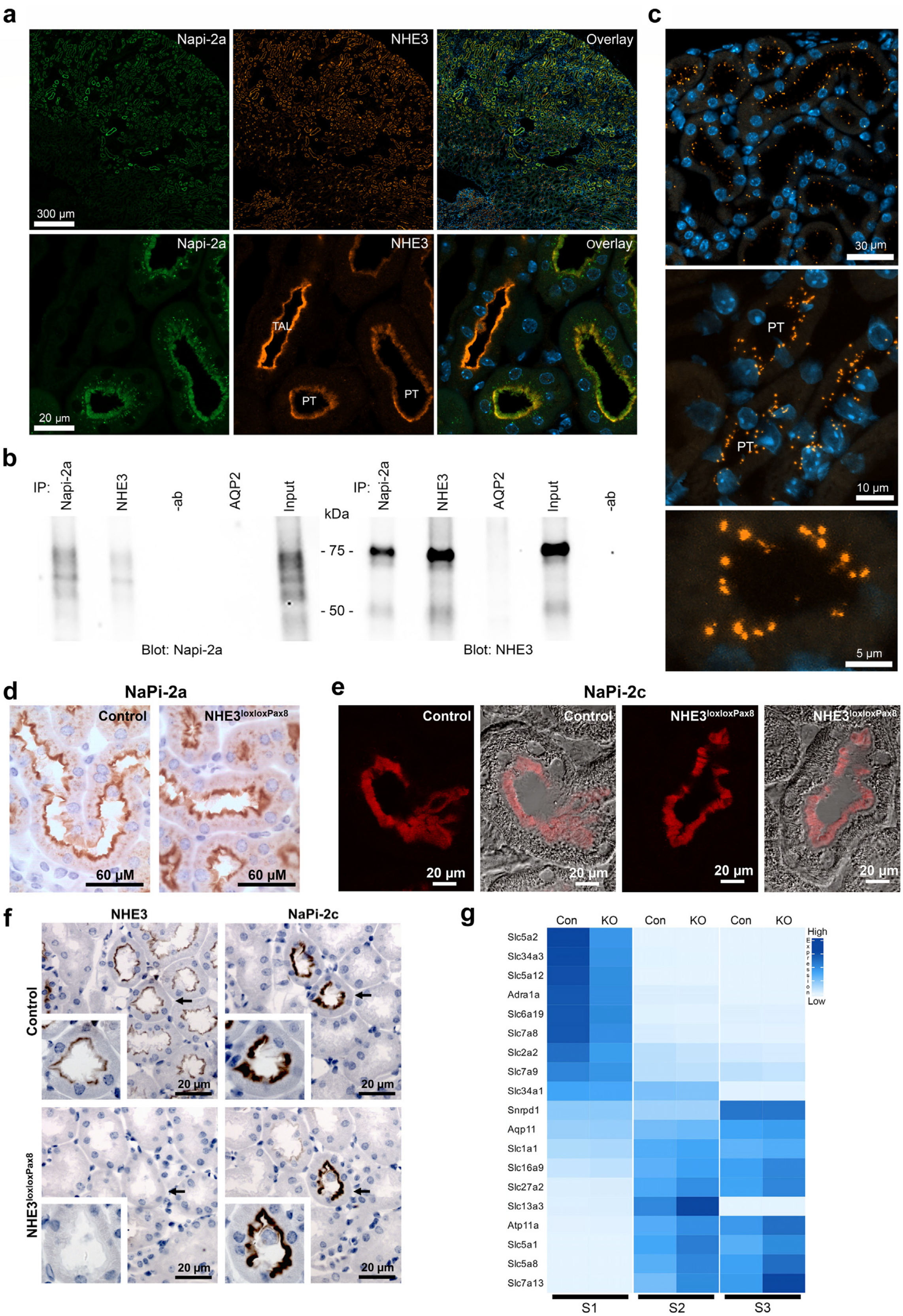

Figure 6 | Gene expression profiling suggests proximal tubule (PT) remodeling in sodium/proton exchanger-3 (NHE3)^{loxloxPax8} mice. (**a**) NHE3 and sodium/phosphate cotransporters-2a (NaPi-2a) at the apical brush border of PT in control mice. (**b**) NaPi-2a and NHE3 can be co-immunoprecipitated in protein lysates from *ex vivo* kidney cortical tubule suspensions. IP = immunoprecipitation antibody, -ab is lysate alone, and input is total protein lysate. (**c**) Proximity ligase assays demonstrate that NHE3 and NaPi-2a are closely associated with (continued)

Acute inhibition of NHE3 using the SGLT2i empagliflozin does not increase urinary Ca^{2+} and P_i excretion

NHE3 and SGLT2 functionally interact in the PT, and lower NHE3 activity subsequent to SGLT2i may underlie, at least in part, their antihypertensive effects.[5–8] SGLT2i may also affect bone metabolism, although these effects are controversial.[62–64] To assess the acute effects of SGLT2i on urinary P_i and Ca^{2+} excretion and a role for NHE3, control and NHE3^{loxloxPax8} mice were treated via oral gavage with vehicle or empagliflozin, and quantitative urine collections performed over 3 hours. Empagliflozin significantly increased glucose excretion in both genotypes, but the increase was smaller in NHE3^{loxloxPax8Cre} mice (Figure 8a). The diuretic and natriuretic effect observed in control mice in response to empagliflozin was absent in NHE3^{loxloxPax8Cre} mice (Figure 8b and c), but urinary P_i, Ca^{2+}, or Cl^- excretion was not altered in either genotype (Figure 8d–f).

DISCUSSION

Drugs that affect kidney NHE3 activity may be useful pharmacologic tools for treating hypertension,[2–4,7,65] and we have previously shown that deletion of NHE3 from the kidney reduces blood pressure.[1] However, the pleotropic effects previously seen after the inhibition of SGLT2 or NaPi-2a suggest that there may be unfavorable side effects after kidney NHE3 inhibition.[36,66] Total NHE3 KO mice have urinary Ca^{2+} wasting and reduced bone mass. Here, we investigated whether Ca^{2+} and P_i homeostasis are altered in mice with genetic deletion of NHE3 specifically in the kidney and the acute effects of SGLT2i on urinary Ca^{2+} and P_i excretion.

A major finding is that relative to controls, NHE3^{loxloxPax8} mice have normal plasma Ca^{2+} and normal urinary Ca^{2+} excretion. This was unexpected considering that approximately 70% of filtered Ca^{2+} is reabsorbed via paracellular transport in the PT in an NHE3-dependent manner.[9–11] However, a role for renal NHE3 in Ca^{2+} handling by the kidney is supported by our results using HTZ, and total NHE3 KO mice have higher urinary Ca^{2+} excretion.[9] So why is Ca^{2+} excretion not changed in the NHE3^{loxloxPax8} mice? One explanation is increased Ca^{2+} reabsorption in the TAL of NHE3^{loxloxPax8} mice, as demonstrated by their greater furosemide-induced calciuresis. The TAL reclaims approximately 25% of Ca^{2+} via paracellular pathways, in a process that is critically dependent on the electrochemical gradient across the TAL and NKCC2 activity.[43,67] Interestingly, the bulk of paracellular Ca^{2+} transport occurs in the more cortical portions of the TAL,[68,69] where we observed greater NKCC2 phosphorylation of S126 (indicating higher activity). This higher NKCC2 activity, coupled with a greater delivery of Na^+ to this segment from the PT in the absence of NHE3, could ultimately increase the lumen-positive potential in the TAL and increase paracellular Ca^{2+} transport by claudin-16 and -19.[67] In addition, NHE3^{loxloxPax8} mice have greater TRPV5 and TRPV6 levels, which should increase Ca^{2+} transport in the DCT. Together, these 2 distal compensatory responses in the NHE3^{loxloxPax8} mice appear to maintain Ca^{2+} homeostasis despite reduced PT Ca^{2+} reabsorption.

We do not have a simple explanation about the factors driving increased NKCC2 and/or TRPV5/6 expression in the NHE3^{loxloxPax8} mice. It may be that higher angiotensin II levels or vasopressin subsequent to volume depletion in the absence of NHE3 is able to stimulate NKCC2,[70,71] although unchanged aldosterone levels in the NHE3^{loxloxPax8} mice would argue against the first possibility.[1] Alternatively, although not reaching significance, the slightly raised PTH levels in the NHE3^{loxloxPax8} mice may be enough to stimulate NKCC2 and put the animals back in Ca^{2+} balance, achieving a new steady state. Another possibility is that, driven by an unknown factor, there is remodeling of the distal nephron to compensate for the major loss of Na^+ from the PT in the absence of NHE3. Remodeling of the PT is supported by our mRNA profiling results (Figure 6g, see later), but whether a concurrent TAL/DCT hypertrophy contributes to increased NKCC2, NaCl cotransporter, and TRPV5/6 would require extensive further investigation using 3-dimensional imaging modalities.

So why do similar compensatory mechanisms not occur in total NHE3 KO mice, which have normal plasma Ca^{2+} but increased urinary Ca^{2+} excretion? Total NHE3 KO mice have a tendency toward reduced plasma PTH,[9] significantly reduced NKCC2,[72] and significantly reduced TRPV5 abundance.[9] These, alongside increased vitD (which reduces plasma PTH levels[73,74]) in total NHE3 KO mice, may explain why the greater Ca^{2+} reabsorption mechanisms observed in the NHE3^{loxloxPax8} mice are absent. Why vitD levels are increased in the total NHE3 KO mice is not clear. One possibility is that they are increased due to a reduced ability of the intestine to absorb Ca^{2+}; however, this increase in vitD would most likely be mediated by hypocalcemia and increased plasma PTH. Alternatively, reduced intestinal P_i absorption in the total NHE3 KO mice may lead to reduced FGF23, and as FGF23 is a potent negative regulator of vitD,[75,76] this may increase vitD levels. Of note, total NHE3 KO mice suffer from congenital sodium diarrhea and volume depletion, making some of the results in this model hard to interpret.

The reduced ability of HTZ to lower urinary Ca^{2+} excretion in NHE3^{loxloxPax8} mice compared with controls supports a role of NHE3 in the PT for Ca^{2+} handling. Three putative different mechanisms exist for the hypocalciuric effect of thiazides. First, thiazides restrict Na^+ entry into DCT cells,

Figure 6 | (continued) punctae (orange) in PTs indicating NHE3:NaPi-2a protein-protein interactions. Cellular localization of (**d**) NaPi-2a and (**e**) NaPi-2c was similar in NHE3^{loxloxPax8} mice relative to controls (n = 6 per genotype). (**f**) Staining of serial sections from NHE3^{loxloxPax8} mice did not detect NHE3 in cells with intact NaPi-2c expression (n = 6 per genotype). (**g**) Heatmap for the mRNA expression of genes associated with the S1 segment of the PT are lower in NHE3^{loxloxPax8} mice than control mice, whereas the expression of genes associated with the S2 and S3 segment are higher. Data in all panels are from male mice. KO, knockout. To optimize viewing of this image, please see the online version of this article at www.kidney-international.org.

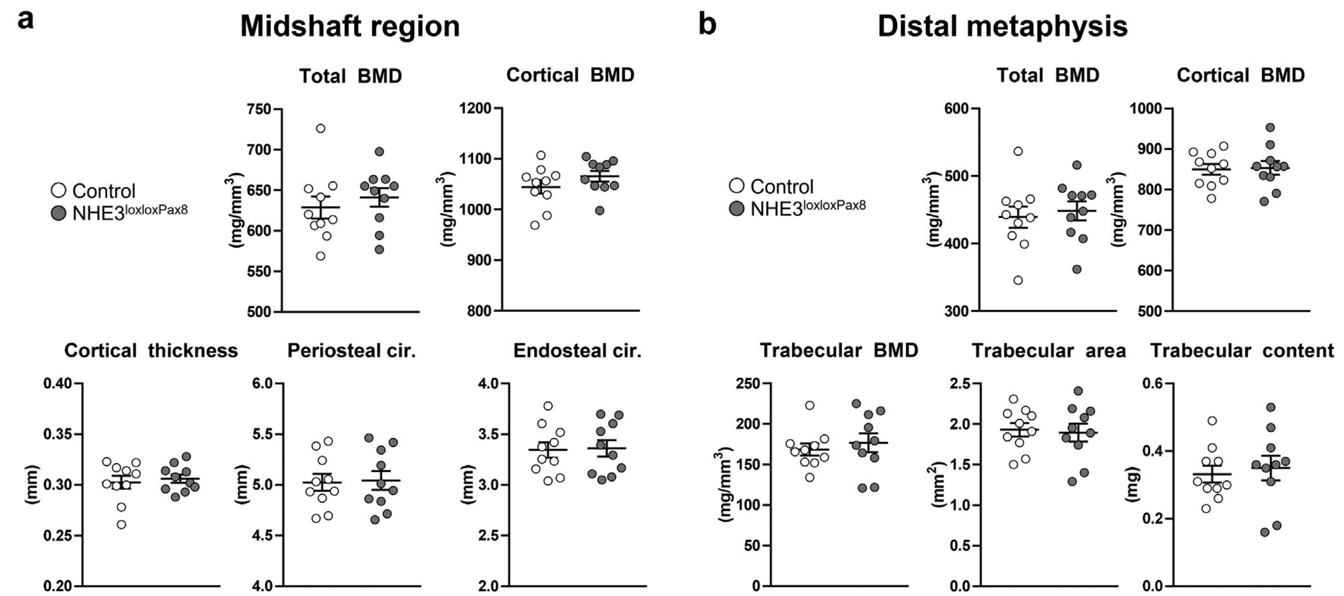

Figure 7 | Loss of kidney sodium/proton exchanger-3 (NHE3) does not result in altered femoral bone mineral density or architecture. (**a**) Peripheral quantitative computed tomography (pQCT) analysis of femur showing total bone mineral density (Total BMD), cortical BMD, cortical thickness, and periosteal and endosteal circumference (cir.) in the midshaft region (n = 10 per genotype). (**b**) Total BMD, cortical BMD, trabecular BMD, trabecular area, and trabecular content in the distal metaphysis region (n = 10 per genotype). Data in all panels are from male mice. Values are mean ± SE and individual data points. Statistical comparisons were performed using appropriate pairwise comparison tests. *$P < 0.05$ versus control.

lowering the intracellular Cl^- concentration and subsequently activating TRPV5.[38–40] However, because HTZ caused similar levels of hypocalciuria in control and TRPV5 KO mice,[12] this mechanism seems unlikely. Secondly, lower intracellular Na^+ concentrations stimulate Ca^{2+} exit across the basolateral membrane via a basolateral Na^+/Ca^{2+} exchanger.[12,40,77] Thirdly, volume depletion in response to thiazides increases NHE3-mediated PT Na^+ reabsorption, thus increasing paracellular Ca^{2+} reabsorption.[12,37] Our data strongly support the last mechanism, but we cannot rule out that the ability of HTZ to stimulate Ca^{2+} reabsorption in the DCT is lower in NHE3^{loxloxPax8} mice because they already have increased Ca^{2+} transport activity in this segment.

Another major finding in this study was that renal NHE3 deletion results in slightly lower NaPi-2a, but greatly reduced NaPi-2c levels. The reduction in NaPi-2a and -2c in NHE3^{loxloxPax8} mice cannot be easily explained by the minor elevation in PTH levels in the NHE3^{loxloxPax8} mice causing NaPi-2a and -2c internalization and degradation,[26,78–82] as one would predict similar and not preferential reductions in NaPi-2a and -2c.[55,82] Furthermore, although we determined that NHE3 and NaPi-2a interact (technical issues prevented us from examining NaPi-2c), no clear differences in NaPi-2a and -2c subcellular localization could be observed between the genotypes and NaPi-2c was undetectable in some cells that expressed NHE3, appearing to preclude alterations in NaPi-2a and -2c distribution, and degradation kinetics[54,55] occur in the absence of NHE3. The most likely explanation for the reduction in NaPi-2a and -2c is PT remodeling. The greater reduction in NaPi-2c relative to NaPi-2a suggests less PT S1 segments, where NaPi-2c is predominantly expressed,[55,59–61,83] which may be counterbalanced by an increase in S2/S3 segments or the distal tubule. This possibility is supported by our reverse transcription quantitative polymerase chain reaction results, where, in general, expression of genes associated with the S1 segment are lower, but genes associated with the S2 and S3 segments are higher in NHE3^{loxloxPax8} mice, and by our observations that in the NHE3^{loxloxPax8} mice, there is lower NaPi-2c mRNA/protein that does not return to the levels seen in control mice during low-P_i diet.

Why, despite the reduced abundances of NaPi-2a and -2c in NHE3^{loxloxPax8} mice, was PT P_i transport not impaired resulting in greater urinary P_i excretion? The likely explanation is the different relative contributions of NaPi-2a and -2c to P_i balance in rodents. Approximately 75% of P_i transport in the mouse kidney is attributed to NaPi-2a, with constitutive NaPi-2a KO mice having hypophosphatemia and increased urinary P_i excretion relative to controls.[84,85] In contrast, the contribution of NaPi-2c to kidney Pi reabsorption is less, with mice lacking NaPi-2c having normal P_i homeostasis and mice with KO of both NaPi-2a and -2c not having greater urinary P_i excretion than NaPi-2a alone deficient mice.[86,87] Hence, the large (approximately 85%) reduction in NaPi-2c relative to the small (approximately 25%) reduction in NaPi-2a in NHE3^{loxloxPax8} mice likely has minimal effects on kidney P_i handling as confirmed by our BBMV and clearance experiments. In perspective, in humans NaPi-2c appears to be the dominant renal P_i handling pathway, with hypophosphatemic rickets with hypercalciuria resulting from homozygous or compound heterozygous

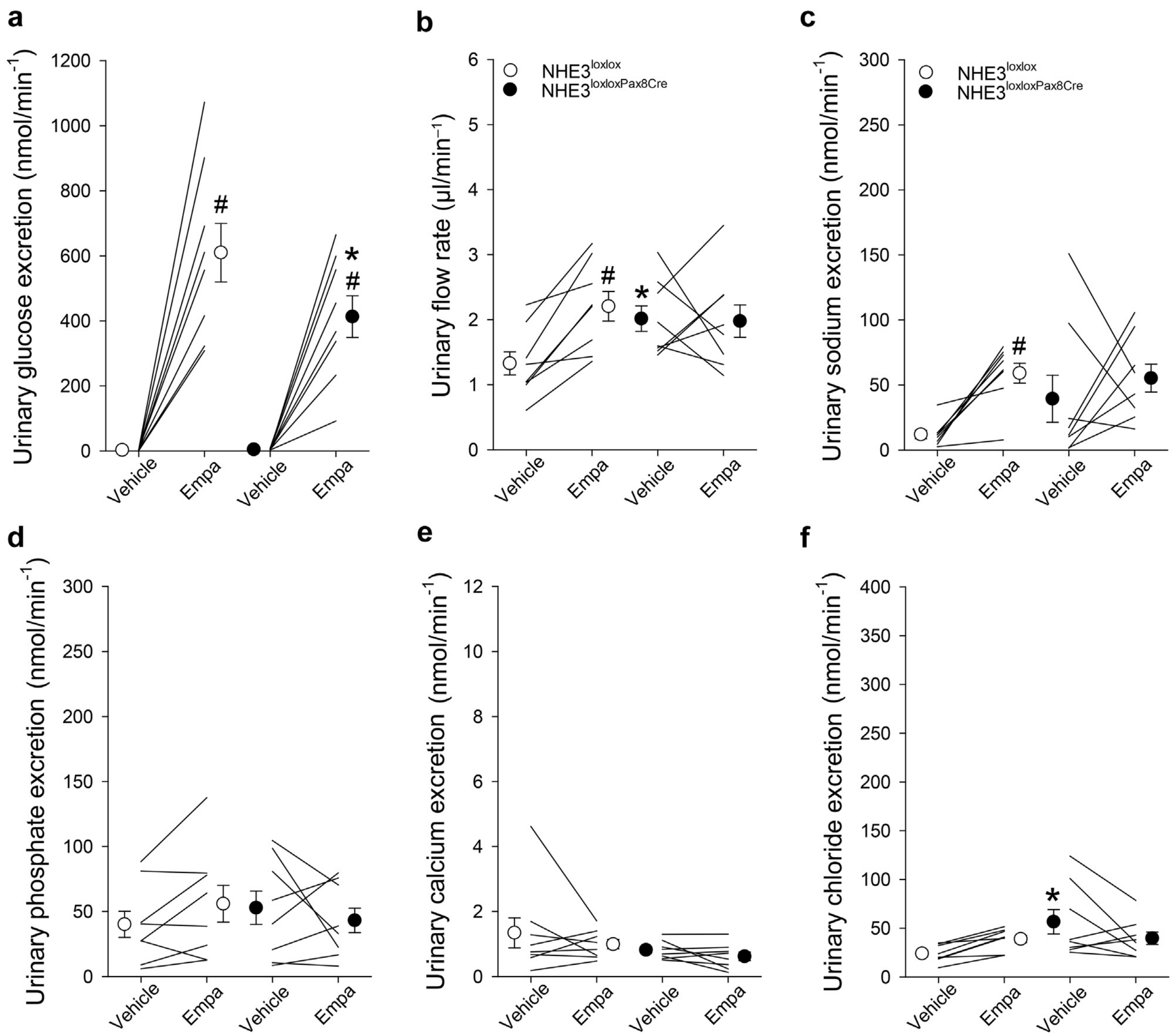

Figure 8 | Acute inhibition of sodium/proton exchanger-3 (NHE3) using the sodium-glucose transporter 2 (SGLT2i) empagliflozin does not increase urinary Ca^{2+} and P_i excretion. Urine was collected over a 3-hour period subsequent to oral gavage of vehicle or empagliflozin. (**a**) Empagliflozin significantly increased glucose excretion in both genotypes, but the increase was smaller in NHE3^{loxloxPax8Cre} mice. (**b**) Empagliflozin significantly increased urine flow and urine Na^+ excretion (**c**) in control mice, but this response was absent in NHE3^{loxloxPax8Cre} mice. Empagliflozin did not alter urinary Ca^{2+} (**d**), P_i (**e**), or Cl^- (**f**) excretion in either genotype. $^{\#}P < 0.05$ versus vehicle same genotype, $^{*}P < 0.05$ versus control same treatment. Data were analyzed by 2-way mixed-effects analysis of variance followed by the 2-stage linear step-up procedure of Benjamini, Krieger, and Yekutieli.

mutations in the *SLC34A3* gene encoding NaPi-2c.[88,89] Therefore, whether orally absorbable NHE3 inhibitors such as AVE0657[3,90] could be used clinically without P_i balance disorders remains an open question.

In contrast to NHE3^{loxloxPax8} mice, global NHE3 KO mice have reduced urinary P_i excretion and normal plasma P_i levels.[9] The difference in urinary P_i excretion may be a result of increased NaPi-2a in the kidneys of total NHE3 KO mice,[72] in contrast to the reduced levels observed in NHE3^{loxloxPax8} mice. These higher levels of NaPi-2a in global NHE3 KO mice may be required to increase renal P_i absorption and keep plasma P_i normal in compensation for reduced intestinal P_i reabsorption. This mechanism is supported by the trend for lower plasma PTH in total NHE3 KO mice.[9] Furthermore, the higher vitD levels in the global NHE3 KO mice may explain why they have reduced bone mass,[9] with enhanced vitD promoting bone resorption. Alternatively, reduced plasma FGF-23 may increase renal NaPi, and although this has not been assessed in NHE3 KO mice, it is supported by tenapanor (nonabsorbable intestinal NHE3 inhibitor) reducing plasma P_i and FGF23 levels.[91] However, inducible intestine-specific NHE3 KO mice show increased and not reduced intestinal P_i transport suggesting species differences.[92]

In conclusion, we demonstrate that despite approximately 70% of filtered Ca^{2+} being reabsorbed in the PT in an NHE3-dependent manner, kidney tubule–specific deletion of NHE3 has no major impact on Ca^{2+} homeostasis. Kidney NHE3 deletion also reduces NaPi-2a and -2c expression, but overall this does not alter P_i balance. Importantly, the large reductions in NaPi-2c observed in $NHE3^{loxloxPax8}$ mice may be relevant for P_i homeostasis in humans if treated with drugs affecting NHE3 activity such as NHE3 inhibitors or gliflozins.

DISCLOSURE

All the authors declared no competing interests.

DATA STATEMENT

There are no data to share that are not already included within the manuscript and Supplementary Material.

ACKNOWLEDGMENTS

We thank Inger Merete S. Paulsen, Helle Høyer, Tina Drejer, Inger Nissen, and Christian V. Westberg for technical assistance. Qi Wu is thanked for generating the heatmaps of gene transcription. The contents do not represent the views of the US Department of Veterans Affairs or the United States Government.

FUNDING

RAF was funded by the Novo Nordisk Foundation (NNF21OC0067647, NNF17OC0028812, NNF20OC0063837, and NNF19OC0058439) and the Independent Research Fund Denmark (0134-00018B). TR was supported by a VA Merit Review Award IBX004968A. HD was funded by the Independent Research Fund Denmark (8045-00011B). AA was supported by a MSCA Post-Doctoral Fellowship Project 101105368.

AUTHOR CONTRIBUTIONS

SBP, SKM, TR, and RAF designed research. SBP, SKM, LT, LLR, AA, RN, HD, TR, and RAF performed and interpreted the results of experiments. SBP, SKM, TR, and RAF prepared figures and drafted the manuscript. SBP, SKM, LT, LLR, AA, RN, HD, TR, and RAF edited and approved the final version of the manuscript.

Supplementary material is available online at www.kidney-international.org.

REFERENCES

1. Fenton RA, Poulsen SB, de la Mora Chavez S, et al. Renal tubular NHE3 is required in the maintenance of water and sodium chloride homeostasis. *Kidney Int*. 2017;92:397–414.
2. Li XC, Soleimani M, Zhu D, et al. Proximal tubule-specific deletion of the NHE3 (Na(+)/H(+) exchanger 3) promotes the pressure-natriuresis response and lowers blood pressure in mice. *Hypertension*. 2018;72: 1328–1336.
3. Li XC, Zhu D, Chen X, et al. Proximal tubule-specific deletion of the NHE3 (Na(+)/H(+) exchanger 3) in the kidney attenuates Ang II (angiotensin II)-induced hypertension in mice. *Hypertension*. 2019;74:526–535.
4. Zhuo JL, Soleimani M, Li XC. New insights into the critical importance of intratubular Na(+)/H(+) exchanger 3 and its potential therapeutic implications in hypertension. *Curr Hypertens Rep*. 2021;23:34.
5. Vallon V. How can inhibition of glucose and sodium transport in the early proximal tubule protect the cardiorenal system? *Nephrol Dial Transplant*. 2024;39:1565–1573.
6. Packer M, Wilcox CS, Testani JM. Critical analysis of the effects of SGLT2 inhibitors on renal tubular sodium, water and chloride homeostasis and their role in influencing heart failure outcomes. *Circulation*. 2023;148: 354–372.
7. Onishi A, Fu Y, Patel R, et al. A role for tubular Na(+)/H(+) exchanger NHE3 in the natriuretic effect of the SGLT2 inhibitor empagliflozin. *Am J Physiol Renal Physiol*. 2020;319:F712–F728.
8. Polidoro J, Osorio N, Girardi A. Physical and functional interaction between NHE3 and SGLT2 in the renal proximal tubule of male and female rats. *Physiology*. 2024;39. https://doi.org/10.1152/physiol.2024.39.S1.2609
9. Pan W, Borovac J, Spicer Z, et al. The epithelial sodium/proton exchanger, NHE3, is necessary for renal and intestinal calcium (re) absorption. *Am J Physiol Renal Physiol*. 2012;302:F943–F956.
10. Blaine J, Chonchol M, Levi M. Renal control of calcium, phosphate, and magnesium homeostasis. *Clin J Am Soc Nephrol*. 2015;10:1257–1272.
11. Alexander RT, Dimke H. Effect of diuretics on renal tubular transport of calcium and magnesium. *Am J Physiol Renal Physiol*. 2017;312: F998–F1015.
12. Nijenhuis T, Vallon V, van der Kemp AW, et al. Enhanced passive Ca^{2+} reabsorption and reduced Mg^{2+} channel abundance explains thiazide-induced hypocalciuria and hypomagnesemia. *J Clin Invest*. 2005;115: 1651–1658.
13. Zhang Y, Norian JM, Magyar CE, et al. In vivo PTH provokes apical NHE3 and NaPi2 redistribution and Na-K-ATPase inhibition. *Am J Physiol*. 1999;276:F711–F719.
14. Bezerra CN, Girardi AC, Carraro-Lacroix LR, et al. Mechanisms underlying the long-term regulation of NHE3 by parathyroid hormone. *Am J Physiol Renal Physiol*. 2008;294:F1232–F1237.
15. Girardi AC, Titan SM, Malnic G, et al. Chronic effect of parathyroid hormone on NHE3 expression in rat renal proximal tubules. *Kidney Int*. 2000;58:1623–1631.
16. Leong PK, Yang LE, Lin HW, et al. Acute hypotension induced by aortic clamp vs. PTH provokes distinct proximal tubule Na+ transporter redistribution patterns. *Am J Physiol Regul Integr Comp Physiol*. 2004;287: R878–R885.
17. Collazo R, Fan L, Hu MC, et al. Acute regulation of Na+/H+ exchanger NHE3 by parathyroid hormone via NHE3 phosphorylation and dynamin-dependent endocytosis. *J Biol Chem*. 2000;275:31601–31608.
18. Mori Y, Machida T, Miyakawa S, et al. Effects of amiloride on distal renal tubule sodium and calcium absorption: dependence on luminal pH. *Pharmacol Toxicol*. 1992;70:201–204.
19. Marone CC, Wong NL, Sutton RA, et al. Effects of metabolic alkalosis on calcium excretion in the conscious dog. *J Lab Clin Med*. 1983;101: 264–273.
20. Sutton RA, Wong NL, Dirks JH. Effects of metabolic acidosis and alkalosis on sodium and calcium transport in the dog kidney. *Kidney Int*. 1979;15: 520–533.
21. Song L. Calcium and bone metabolism indices. *Adv Clin Chem*. 2017;82: 1–46.
22. Rizzoli R, Fleisch H, Bonjour JP. Role of 1,25-dihydroxyvitamin D3 on intestinal phosphate absorption in rats with a normal vitamin D supply. *J Clin Invest*. 1977;60:639–647.
23. Christensen EI, Verroust PJ, Nielsen R. Receptor-mediated endocytosis in renal proximal tubule. *Pflugers Arch*. 2009;458:1039–1048.
24. Capuano P, Bacic D, Roos M, et al. Defective coupling of apical PTH receptors to phospholipase C prevents internalization of the Na+-phosphate cotransporter NaPi-IIa in Nherf1-deficient mice. *Am J Physiol Cell Physiol*. 2007;292:C927–C934.
25. Deliot N, Hernando N, Horst-Liu Z, et al. Parathyroid hormone treatment induces dissociation of type IIa Na+-P(i) cotransporter-Na+/H+ exchanger regulatory factor-1 complexes. *Am J Physiol Cell Physiol*. 2005;289:C159–C167.
26. Lanzano L, Lei T, Okamura K, et al. Differential modulation of the molecular dynamics of the type IIa and IIc sodium phosphate cotransporters by parathyroid hormone. *Am J Physiol Cell Physiol*. 2011;301:C850–C861.
27. Lederer ED, Khundmiri SJ, Weinman EJ. Role of NHERF-1 in regulation of the activity of Na-K ATPase and sodium-phosphate co-transport in epithelial cells. *J Am Soc Nephrol*. 2003;14:1711–1719.
28. Madjdpour C, Bacic D, Kaissling B, et al. Segment-specific expression of sodium-phosphate cotransporters NaPi-IIa and -IIc and interacting proteins in mouse renal proximal tubules. *Pflugers Arch*. 2004;448:402–410.
29. Mahon MJ, Segre GV. Stimulation by parathyroid hormone of a NHERF-1-assembled complex consisting of the parathyroid hormone I receptor, phospholipase Cbeta, and actin increases intracellular calcium in opossum kidney cells. *J Biol Chem*. 2004;279:23550–23558.
30. Murer H, Hernando N, Forster I, et al. Regulation of Na/Pi transporter in the proximal tubule. *Annu. Rev. Physiol*. 2003;65:531–542.
31. Kung CJ, Haykir B, Schnitzbauer U, et al. Fibroblast growth factor 23 (FGF23) leads to endolysosomal routing of the renal phosphate

co-transporters NaPi-IIa and NaPi-IIc in vivo. *Am J Physiol Renal Physiol*. 2021;321:F785–F798.
32. Lanske B, Razzaque MS. Molecular interactions of FGF23 and PTH in phosphate regulation. *Kidney Int*. 2014;86:1072–1074.
33. Yang LE, Maunsbach AB, Leong PK, et al. Differential traffic of proximal tubule Na+ transporters during hypertension or PTH: NHE3 to base of microvilli vs. NaPi2 to endosomes. *Am J Physiol Renal Physiol*. 2004;287: F896–F906.
34. Thomson RB, Wang T, Thomson BR, et al. Role of PDZK1 in membrane expression of renal brush border ion exchangers. *Proc Natl Acad Sci U S A*. 2005;102:13331–13336.
35. Fenton RA, Poulsen SB, de la Mora Chavez S, et al. Caffeine-induced diuresis and natriuresis is independent of renal tubular NHE3. *Am J Physiol Renal Physiol*. 2015;308:F1409–F1420.
36. Thomas L, Xue J, Murali SK, et al. Pharmacological Npt2a inhibition causes phosphaturia and reduces plasma phosphate in mice with normal and reduced kidney function. *J Am Soc Nephrol*. 2019;30:2128–2139.
37. Nijenhuis T, Hoenderop JG, Loffing J, et al. Thiazide-induced hypocalciuria is accompanied by a decreased expression of Ca2+ transport proteins in kidney. *Kidney Int*. 2003;64:555–564.
38. Costanzo LS. Localization of diuretic action in microperfused rat distal tubules: Ca and Na transport. *Am J Physiol*. 1985;248:F527–F535.
39. Gesek FA, Friedman PA. Mechanism of calcium transport stimulated by chlorothiazide in mouse distal convoluted tubule cells. *J Clin Invest*. 1992;90:429–438.
40. Friedman PA. Codependence of renal calcium and sodium transport. *Annu Rev Physiol*. 1998;60:179–197.
41. Marneros AG. Magnesium and calcium homeostasis depend on KCTD1 function in the distal nephron. *Cell Rep*. 2021;34:108616.
42. Eveloff JL, Calamia J. Effect of osmolarity on cation fluxes in medullary thick ascending limb cells. *Am J Physiol*. 1986;250:F176–F180.
43. Di Stefano A, Roinel N, de Rouffignac C, et al. Transepithelial Ca2+ and Mg2+ transport in the cortical thick ascending limb of Henle's loop of the mouse is a voltage-dependent process. *Ren Physiol Biochem*. 1993;16: 157–166.
44. Ortiz PA. cAMP increases surface expression of NKCC2 in rat thick ascending limbs: role of VAMP. *Am J Physiol Renal Physiol*. 2006;290: F608–F616.
45. Gimenez I, Forbush B. Short-term stimulation of the renal Na-K-Cl cotransporter (NKCC2) by vasopressin involves phosphorylation and membrane translocation of the protein. *J Biol Chem*. 2003;278:26946–26951.
46. Gunaratne R, Braucht DW, Rinschen MM, et al. Quantitative phosphoproteomic analysis reveals cAMP/vasopressin-dependent signaling pathways in native renal thick ascending limb cells. *Proc Natl Acad Sci U S A*. 2010;107:15653–15658.
47. Dimke H, Griveau C, Ling WE, et al. Claudin-19 localizes to the thick ascending limb where its expression is required for junctional claudin-16 localization. *Ann N Y Acad Sci*. 2023;1526:126–137.
48. Prot-Bertoye C, Griveau C, Skjodt K, et al. Differential localization patterns of claudin 10, 16, and 19 in human, mouse, and rat renal tubular epithelia. *Am J Physiol Renal Physiol*. 2021;321:F207–F224.
49. van Megen WH, Tan RSG, Alexander RT, et al. Differential parathyroid and kidney Ca(2+)-sensing receptor activation in autosomal dominant hypocalcemia 1. *EBioMedicine*. 2022;78:103947.
50. Frische S, Alexander RT, Ferreira P, et al. Localization and regulation of claudin-14 in experimental models of hypercalcemia. *Am J Physiol Renal Physiol*. 2021;320:F74–F86.
51. Szczepanska-Konkel M, Yusufi AN, VanScoy M, et al. Phosphonocarboxylic acids as specific inhibitors of Na+-dependent transport of phosphate across renal brush border membrane. *J Biol Chem*. 1986;261:6375–6383.
52. Donowitz M, Cha B, Zachos NC, et al. NHERF family and NHE3 regulation. *J Physiol*. 2005;567:3–11.
53. Donowitz M, Li X. Regulatory binding partners and complexes of NHE3. *Physiol Rev*. 2007;87:825–872.
54. Fenton RA, Murray F, Dominguez Rieg JA, et al. Renal phosphate wasting in the absence of adenylyl cyclase 6. *J Am Soc Nephrol*. 2014;25:2822–2834.
55. Picard N, Capuano P, Stange G, et al. Acute parathyroid hormone differentially regulates renal brush border membrane phosphate cotransporters. *Pflugers Arch*. 2010;460:677–687.
56. Alam MS. Proximity ligation assay (PLA). *Methods Mol Biol*. 2022;2422: 191–201.
57. Layton AT, Vallon V. SGLT2 inhibition in a kidney with reduced nephron number: modeling and analysis of solute transport and metabolism. *Am J Physiol Renal Physiol*. 2018;314:F969–F984.
58. Rieg T, Masuda T, Gerasimova M, et al. Increase in SGLT1-mediated transport explains renal glucose reabsorption during genetic and pharmacological SGLT2 inhibition in euglycemia. *Am J Physiol Renal Physiol*. 2014;306:F188–F193.
59. Wu H, Kirita Y, Donnelly EL, et al. Advantages of single-nucleus over single-cell RNA sequencing of adult kidney: rare cell types and novel cell states revealed in fibrosis. *J Am Soc Nephrol*. 2019;30:23–32.
60. Chen L, Chou CL, Yang CR, et al. Multiomics analyses reveal sex differences in mouse renal proximal subsegments. *J Am Soc Nephrol*. 2023;34:829–845.
61. Chen L, Chou CL, Knepper MA. A comprehensive map of mRNAs and their isoforms across all 14 renal tubule segments of mouse. *J Am Soc Nephrol*. 2021;32:897–912.
62. Ye Y, Zhao C, Liang J, et al. Effect of sodium-glucose co-transporter 2 inhibitors on bone metabolism and fracture risk. *Front Pharmacol*. 2018;9:1517.
63. Ko HY, Bea S, Jeong HE, et al. Sodium-glucose cotransporter 2 inhibitors vs incretin-based drugs and risk of fractures for type 2 diabetes. *JAMA Netw Open*. 2023;6:e2335797.
64. Zhang YS, Zheng YD, Yuan Y, et al. Effects of anti-diabetic drugs on fracture risk: a systematic review and network meta-analysis. *Front Endocrinol (Lausanne)*. 2021;12:735824.
65. Borges-Junior FA, Silva Dos Santos D, Benetti A, et al. Empagliflozin inhibits proximal tubule NHE3 activity, preserves GFR, and restores euvolemia in nondiabetic rats with induced heart failure. *J Am Soc Nephrol*. 2021;32:1616–1629.
66. Vallon V, Verma S. Effects of SGLT2 inhibitors on kidney and cardiovascular function. *Annu Rev Physiol*. 2021;83:503–528.
67. Alexander RT, Dimke H. Molecular mechanisms underlying paracellular calcium and magnesium reabsorption in the proximal tubule and thick ascending limb. *Ann N Y Acad Sci*. 2022;1518:69–83.
68. Suki WN, Rouse D, Ng RC, et al. Calcium transport in the thick ascending limb of Henle. Heterogeneity of function in the medullary and cortical segments. *J Clin Invest*. 1980;66:1004–1009.
69. Bleich M, Wulfmeyer VC, Himmerkus N, et al. Heterogeneity of tight junctions in the thick ascending limb. *Ann N Y Acad Sci*. 2017;1405:5–15.
70. Nguyen MT, Lee DH, Delpire E, et al. Differential regulation of Na+ transporters along nephron during ANG II-dependent hypertension: distal stimulation counteracted by proximal inhibition. *Am J Physiol Renal Physiol*. 2013;305:F510–F519.
71. Rieg T, Tang T, Uchida S, et al. Adenylyl cyclase 6 enhances NKCC2 expression and mediates vasopressin-induced phosphorylation of NKCC2 and NCC. *Am J Pathol*. 2013;182:96–106.
72. Brooks HL, Sorensen AM, Terris J, et al. Profiling of renal tubule Na+ transporter abundances in NHE3 and NCC null mice using targeted proteomics. *J Physiol*. 2001;530:359–366.
73. Silver J, Yalcindag C, Sela-Brown A, et al. Regulation of the parathyroid hormone gene by vitamin D, calcium and phosphate. *Kidney Int Suppl*. 1999;73:S2–S7.
74. Banon S, Rosillo M, Gomez A, et al. Effect of a monthly dose of calcidiol in improving vitamin D deficiency and secondary hyperparathyroidism in HIV-infected patients. *Endocrine*. 2015;49:528–537.
75. Murali SK, Roschger P, Zeitz U, et al. FGF23 Regulates bone mineralization in a 1,25(OH)2 D3 and Klotho-independent manner. *J Bone Miner Res*. 2016;31:129–142.
76. Insogna KL, Briot K, Imel EA, et al. A randomized, double-blind, placebo-controlled, phase 3 trial evaluating the efficacy of burosumab, an anti-FGF23 antibody, in adults with X-linked hypophosphatemia: week 24 primary analysis. *J Bone Miner Res*. 2018;33:1383–1393.
77. Friedman PA, Bushinsky DA. Diuretic effects on calcium metabolism. *Semin Nephrol*. 1999;19:551–556.
78. Levi M, Gratton E. Visualizing the regulation of SLC34 proteins at the apical membrane. *Pflugers Arch*. 2019;471:533–542.
79. Pfister MF, Ruf I, Stange G, et al. Parathyroid hormone leads to the lysosomal degradation of the renal type II Na/Pi cotransporter. *Proc Natl Acad Sci U S A*. 1998;95:1909–1914.
80. Segawa H, Yamanaka S, Onitsuka A, et al. Parathyroid hormone-dependent endocytosis of renal type IIc Na-Pi cotransporter. *Am J Physiol Renal Physiol*. 2007;292:F395–F403.

81. Giral H, Lanzano L, Caldas Y, et al. Role of PDZK1 protein in apical membrane expression of renal sodium-coupled phosphate transporters. *J Biol Chem*. 2011;286:15032–15042.
82. Segawa H, Yamanaka S, Ito M, et al. Internalization of renal type IIc Na-Pi cotransporter in response to a high-phosphate diet. *Am J Physiol Renal Physiol*. 2005;288:F587–F596.
83. Breusegem SY, Takahashi H, Giral-Arnal H, et al. Differential regulation of the renal sodium-phosphate cotransporters NaPi-IIa, NaPi-IIc, and PiT-2 in dietary potassium deficiency. *Am J Physiol Renal Physiol*. 2009;297: F350–F361.
84. Beck L, Karaplis AC, Amizuka N, et al. Targeted inactivation of Npt2 in mice leads to severe renal phosphate wasting, hypercalciuria, and skeletal abnormalities. *Proc Natl Acad Sci U S A*. 1998;95: 5372–5377.
85. Thomas L, Xue J, Tomilin VN, et al. PF-06869206 is a selective inhibitor of renal P(i) transport: evidence from in vitro and in vivo studies. *Am J Physiol Renal Physiol*. 2020;319:F541–F551.
86. Myakala K, Motta S, Murer H, et al. Renal-specific and inducible depletion of NaPi-IIc/Slc34a3, the cotransporter mutated in HHRH, does not affect phosphate or calcium homeostasis in mice. *Am J Physiol Renal Physiol*. 2014;306:F833–F843.
87. Segawa H, Onitsuka A, Furutani J, et al. Npt2a and Npt2c in mice play distinct and synergistic roles in inorganic phosphate metabolism and skeletal development. *Am J Physiol Renal Physiol*. 2009;297:F671–F678.
88. Wagner CA, Rubio-Aliaga I, Hernando N. Renal phosphate handling and inherited disorders of phosphate reabsorption: an update. *Pediatr Nephrol*. 2019;34:549–559.
89. Gattineni J, Baum M. Genetic disorders of phosphate regulation. *Pediatr Nephrol*. 2012;27:1477–1487.
90. European Union Clinical Trials Registry, Eudra CT Number 2007-002174-58. https://www.clinicaltrialsregister.eu
91. Labonte ED, Carreras CW, Leadbetter MR, et al. Gastrointestinal inhibition of sodium-hydrogen exchanger 3 reduces phosphorus absorption and protects against vascular calcification in CKD. *J Am Soc Nephrol*. 2015;26: 1138–1149.
92. Xue J, Thomas L, Murali SK, et al. Enhanced phosphate absorption in intestinal epithelial cell-specific NHE3 knockout mice. *Acta Physiol (Oxf)*. 2022:e13756.